Molecular Crystals and Liquid Crystals Incorporating Nonlinear Optics

Publication details, including instructions for authors and subscription information:
http://www.tandfonline.com/loi/gmcl17

On the Polarization Electric Field in Surface-Stabilized Ferroelectric Liquid Crystalst

M. Nakagawa [a]

[a] Department of Electrical Engineering, Faculty of Engineering, Nagaoka University of Technology, Nagaoka, Niigata, 940-21, Japan

Version of record first published: 22 Sep 2006.

To cite this article: M. Nakagawa (1989): On the Polarization Electric Field in Surface-Stabilized Ferroelectric Liquid Crystalst, Molecular Crystals and Liquid Crystals Incorporating Nonlinear Optics, 173:1, 1-16

To link to this article: http://dx.doi.org/10.1080/00268948908033363

Mol. Cryst. Liq. Cryst., 1989, Vol. 173, pp. 1–16
Reprints available directly from the publisher
Photocopying permitted by license only

Printed in the United States of America

On the Polarization Electric Field in Surface-Stabilized Ferroelectric Liquid Crystals†

M. NAKAGAWA

Department of Electrical Engineering, Faculty of Engineering, Nagaoka University of Technology, Nagaoka, Niigata 940-21, Japan

(*Received August 15, 1988; in final form February 10, 1989*)

In this work, some basic effects of polarization electric field on dynamic behavior of SmC* liquid crystals are examined on the basis of a simple model. Applying a step-like electric field, those effects are investigated with a strongly anchored and also a weakly anchored boundary condition for the *c*-director. From numerical analyses, it is found that the polarization field has a tendency to considerably relax a dynamic response of SmC* under the electric field. With a weakly anchored boundary condition, a double-peaked polarization current is found for an appropriate anchoring strength.

Keywords: ferroelectric liquid crystals, polarization electric field

1. INTRODUCTION

Dynamic behavior of the surface stabilized ferroelectric liquid crystals (SSFLCs) has been studied up to now on the basis of several theoretical models.[1–5] In those studies, a spatially homogeneous electric field has been assumed for simplicity in a distorted SmC* sample under an external field. However, as was recently pointed out by several authors for elastic deformation in SSFLCs[6,7] and for an infinite SmC* system without any boundary,[9] the polarization electric field or an electrostatic interaction between spatially distributed polarization charges may have important influence on the elastic properties of the SmC* especially for a large spontaneous polarization. That is, such effects have a tendency to increase the effective elastic constant, which may be observed as an apparent increase of stiffness of the SmC* in a static problem as was pointed out in the previous works.[6,7] Moreover, for a dynamic problem, an increase of the effective elastic constant may cause an increase of the apparent rotational viscosity as can be easily expected from a torque balance equation. From this aspect, very recently, we studied the dynamic behavior of SSFLC cells under a sinusoidal electric field, and found that the polarization field caused by spatially distributed polarization charges considerably increases the apparent rotational viscosity and critically bears on their polarization switching cur-

† This work was accomplished at the Department of Mathematics, University of Strathclyde, Livingstone Tower, 26 Richmond Street, Glasgow G1 1XH, U.K.

rents as well as the P-E hysteresis curves.[8] Therein we also discussed the significance of symmetry of the anchoring function at the boundaries on the dynamic behavior. Amaya *et al.*[1] utilized a sinusoidal function such as $-g_1\cos^2(\Phi - \Phi_p) - g_2\cos(\Phi - \Phi_p)$ to express an anchoring energy between the SmC* molecules and the bounding plates; here g_1 and g_2 are non-polar and polar interaction strengths between SmC* molecules and a boundary surface, respectively, and Φ and Φ_p stand for an azimuthal angle of the *c*-director and a selective pre-tilt angle measured from a bounding plate, respectively. With this anchoring function, they found a rotating *c*-director under an alternating electric field.[10] As was pointed out by us in the previous work,[8] however, this kind of anchoring function has no mirror symmetry with respect to the plane normal of the bounding plate even for a non-polar surface with a certain selective pre-tilt angle, and is obviously contradict with a real system. In fact, in the previous study, utilizing an anchoring function consistent with such symmetry consideration, an oscillating (not rotating) *c*-director between bounding plates was found under an alternating electric field.[8] Therefore it seems to be significant to reconsider dynamic problems of SmC* making use of an anchoring function consistent with a real system.

From the above-mentioned aspects, in the present work, we shall clarify some basic effects of polarization electric field on a transient behavior under a step-like applied electric field. This kind of problem has been studied in a few somewhat simplified models by several authors.[2–5] This simplification of the applied field will help to make effects of polarization fields apparent. Deriving an explicit expression for the polarization electric field from Poisson's equation, its spatio-temporal behavior will be also presented. In §2 theoretical preliminaries will be reviewed in brief. Then some numerical results will be given in §3. Therein one will find the significance of the polarization field as well as the anchoring at the boundaries. Finally §4 is devoted to mention some concluding remarks related to a spatio-temporal behavior of the polarization field.

§2. THEORETICAL MODEL

In the present work, we shall restrict our interest to a one-dimensional dynamic problem in space similar to our previous work.[8] Therefore all physical variables are assumed to depend on only y and t, where y axis is taken to be normal two parallel bounding plates which are separated by a cell gap d. In addition the z axis is assumed to be coincident with the layer normal. The schematic drawing of the coordinate system is given in Figure 1. First of all, similar to the previous work,[6–8] the free energy density f is assumed to be simply given by

$$\begin{aligned} f = {} & \frac{K}{2}\left[\frac{\partial\Phi}{\partial y}\right]^2 + Kq\sin\Phi\frac{\partial\Phi}{\partial y} \\ & - \frac{\epsilon}{2}\left[\frac{\partial\Psi}{\partial y}\right]^2 + P_s\cos\Phi\frac{\partial\Psi}{\partial y} \\ & + f_s^0\delta(y) + f_s^d\delta(y-d), \end{aligned} \tag{1}$$

where K is an elastic constant, Φ is an azimuthal angle of the c-director measured from the bounding plate as shown in Figure 1, q is a wave number concerned with the inherent chirality perpendicular to the layer normal, ϵ is a dielectric constant, Ψ is an electric scalar potential, P_s is a spontaneous polarization, f_s^0 and f_s^d are the surface anchoring energies per unit area at $y = 0$ and $y = d$, respectively, assumed to be given by

$$f_s^0(\Phi) = -\frac{g^0}{2}[\exp[-\alpha \sin^2\{(\Phi - \Phi_0)/2\}] + \exp[-\alpha \cos^2\{(\Phi + \Phi_0)/2\}]], (y = 0) \quad (2a)$$

and

$$f_s^d(\Phi) = -\frac{g^d}{2}[\exp[-\alpha \sin^2\{(\Phi - \Phi_d)/2\}] + \exp[-\alpha \cos^2\{(\Phi + \Phi_d)/2\}]], (y = d) \quad (2b)$$

respectively; here g^0 and g^d are anchoring strengths at $y = 0$ and $y = d$, respectively, and α represents a steepness of the anchoring potential, Φ_0 and Φ_d are concerned with selective pre-tilt angles at $y = 0$ and $y = d$, respectively.[8] Here we assumed that the anisotropies of elastic and dielectric constants could be neglected, and that the surface interaction has no polarity.[8] It may be noticeable to see in Equations (2a) and (2b) that $f_s^{0,d}(\Phi) = f_s^{0,d}(\pi - \Phi)$ consistent with the symmetry argument.[8] Then the free energy per unit area F can be given by

$$F = \int_0^d dy\, f. \quad (3)$$

Now the torque balance equations of the c-director and the Poisson's equation in order to determine the internal electric field can be derived as[8]

$$\gamma \frac{\partial \Phi}{\partial t} = -\frac{\delta F}{\delta \Phi} = -\frac{\partial f}{\partial \Phi} + \frac{\partial}{\partial y}\frac{\partial f}{\partial(\partial \Phi/\partial y)}, \quad (0 < y < d) \quad (4)$$

$$\frac{\partial F}{\partial(\partial \Phi/\partial y)} = \frac{\partial f_s}{\partial \Phi}, \quad (y = 0) \quad (5)$$

$$\frac{\partial F}{\partial(\partial \Phi/\partial y)} = -\frac{\partial f_s}{\partial \Phi}, \quad (y = d) \quad (6)$$

$$\frac{\delta F}{\delta \Psi} = \frac{\partial f}{\partial \Psi} - \frac{\partial}{\partial y}\frac{\partial f}{\partial(\partial \Psi/\partial y)} = 0, \quad (7)$$

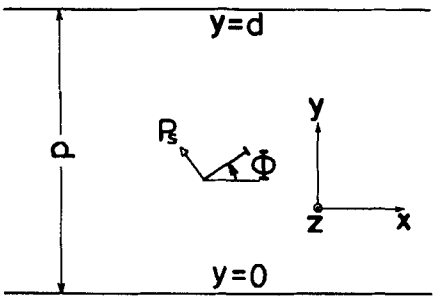

FIGURE 1 The coordinate system for a theoretical formulation. Here y axis is taken to be normal to the bounding plates, and z axis is coincident with the layer normal of the book-shelf geometry.

or substituting Equation (1) to these, one finds

$$\gamma\frac{\partial\Phi}{\partial t} = K\frac{\partial^2\Phi}{\partial y^2} + P_s\sin\Phi\frac{\partial\Psi}{\partial y}, \tag{4a}$$

$$K\frac{\partial\Phi}{\partial y} + Kq\sin\Phi = \frac{\alpha g^0}{4}[\sin(\Phi - \Phi_0)\exp[-\alpha\sin^2\{(\Phi - \Phi_0)/2\}] - \sin(\Phi + \Phi_0)\exp[-\alpha\cos^2\{(\Phi + \Phi_0)/2\}]]\,(y = 0) \tag{5a}$$

$$K\frac{\partial\Phi}{\partial y} + Kq\sin\Phi = -\frac{\alpha g^d}{4}[\sin(\Phi - \Phi_d)\exp[-\alpha\sin^2\{(\Phi - \Phi_d)/2\}] - \sin(\Phi + \Phi_d)\exp[-\alpha\cos^2\{(\Phi + \Phi_d)/2\}]]\,(y = d) \tag{6a}$$

$$\frac{\partial}{\partial y}\left[-\epsilon\frac{\partial\Psi}{\partial y} + P_s\cos\Phi\right] = 0. \tag{7a}$$

These are basic equations to treat dynamic behavior in the present model. In the previous study,[8] (7a) was solved numerically by means of a finite difference method as well as (4a). Alternatively, in the present work, we shall solve (7a) analytically and make the role of the polarization field clear. For this purpose, first integrating (7a), one finds

$$-\epsilon\frac{\partial\Psi}{\partial y} + P_s\cos\Phi = D_y(t), \tag{8}$$

where an integration constant D_y stands for an electric displacement along y and may be a function of time. It should be noted here that the spatial dependences of the internal electric field ($\partial\Psi/\partial y$) and that of polarization ($\cos\Phi$) are canceled

out each other for $0 < y < d$ so that $\partial D_y/\partial y = 0$ (or (7a)). Again integrating (8) over the sample thickness d, one readily finds

$$D_y(t) = \epsilon E(t) + P_s\langle\cos\Phi\rangle, \tag{9}$$

where $\langle\cos\Phi\rangle$ is defined as a spatial average of $\cos\Phi$ over sample thickness as follows

$$\langle\cos\Phi\rangle = \frac{1}{d}\int_0^d dy \cos\Phi(y,t), \tag{10}$$

and $E(t)$ is understood as an externally applied electric field and defined by

$$E(t) = -\frac{\Psi(d,t) - \Psi(0,t)}{d}. \tag{11}$$

In (9) what can be externally controlled in experiments is not $E(t)$ but $D_y(t)$. Therefore measuring the electric displacement current dD_y/dt, and then integrating it with respect to t, we can determine the averaged spontaneous polarization $P_s\langle\cos\Phi\rangle$ from (9). Now, from (8) and (9), one has

$$\frac{\partial\Psi}{\partial y} = -E(t) + \frac{P_s}{\epsilon}(\cos\Phi - \langle\cos\Phi\rangle). \tag{12}$$

Finally, substituting (12) into (4a) to eliminate $\Psi(y, t)$, we have

$$\begin{aligned}\gamma\frac{\partial\Phi}{\partial t} = K\frac{\partial^2\Phi}{\partial y^2} - P_sE(t)\sin\Phi \\ + \frac{P_s^2}{\epsilon}\sin\Phi(\cos\Phi - \langle\cos\Phi\rangle).\end{aligned} \tag{13}$$

where, in the right hand side, the first term represents an elastic restoring torque, the second one does an external one, and the last term corresponds to a contribution from the polarization field. Here introducing the following normalized quantities for convenience,

$$\tau = \frac{K}{\gamma d^2}t, \tag{14a}$$

$$\zeta = \frac{y}{d}, \tag{14b}$$

$$e(\tau) = \frac{d^2}{K}P_sE(t), \tag{14c}$$

$$\Lambda = \frac{(P_sd)^2}{K\epsilon}, \tag{14d}$$

we may rewrite (13) as the following non-linear partial integro-differential equation for Φ.

$$\frac{\partial\Phi}{\partial\tau} = \frac{\partial^2\Phi}{\partial\zeta^2} - \{e(\tau) + e_p(\zeta,\tau)\}\sin\Phi, \tag{15}$$

where $e_p(\zeta,\tau)$ is the polarization field expressed by

$$e_p(\zeta,\tau) = \Lambda(\langle\cos\Phi\rangle - \cos\Phi). \tag{16}$$

According to this explicit expression for e_p, one may see what follows. First one finds that the polarization field results from the difference between a spatially averaged spontaneous polarization proportional to $\langle\cos\Phi\rangle$ and a local one proportional to $\cos\Phi$. Second the strength of polarization field is just proportional to a coupling parameter $\Lambda = (P_s d)^2/(K\epsilon)$, which may be estimated as the order of 100 for $P_s = 10^{-4}C/m^2$ $d = 10^{-6}m$, $K = 10^{-11}N$ and $\epsilon = 10^{-11}$ F/m. From an energetical point of view, since a production of e_p is accompanied with an increase of electrostatic energy due to an interaction between spatially distributed polarization charges,[6,7,9] $\cos\Phi$ tends to be close to $\langle\cos\Phi\rangle$ at any τ ($\tau > 0$) and ζ ($0 < \zeta < 1$) as Λ becomes large. In other words, an increasing Λ results in an apparent increase of an effective elastic constant. Therefore if the surface anchoring is strong enough to fix the director orientation at the boundaries, the rotation of the c-director under an applied field may be slowed and suppressed for large Λ as will be numerically explored in the next section. Next, utilizing (14a)–(14d), the surface torque balance equations read, from (5a) and (6a),

$$\frac{\partial\Phi}{\partial\zeta} + Q\sin\Phi = \frac{G^0}{4}[\sin(\Phi - \Phi_0)\exp[-\alpha\sin^2\{(\Phi - \Phi_0)/2\}] - \sin(\Phi + \Phi_0)\exp[-\alpha\cos^2\{(\Phi + \Phi_0)/2\}]] \quad (y = 0) \tag{17a}$$

$$\frac{\partial\Phi}{\partial\zeta} + Q\sin\Phi = -\frac{G^d}{4}[\sin(\Phi - \Phi_d)\exp[-\alpha\sin^2\{(\Phi - \Phi_d)/2\}] - \sin(\Phi + \Phi_d)\exp[-\alpha\cos^2\{(\Phi + \Phi_d)/2\}]] \quad (y = d) \tag{17b}$$

where Q and $G^{0,d}$ are defined by qd and $(\alpha g^{0,d}d)/K$, respectively.

Finally a reduced polarization current $I_p(\tau)$ may be introduced by

$$I_p(\tau) = \frac{d\langle\cos\Phi\rangle}{d\tau}, \tag{18}$$

which equals an electric displacement current for such a step-like applied field as

$de(\tau)/d\tau = 0$ ($\tau > 0$). Now putting $e(\tau) = -e_m$ ($E(t) = -E_m$) for $\tau > 0$ ($t > 0$), from (14a) and (14c), we have the following relationship.

$$\tau_w e_m = \frac{K}{\gamma d^2} t_w \frac{P_s d^2}{K} E_m$$

$$= \frac{P_s}{\gamma} t_w E_m, \tag{19}$$

or

$$t_w = (\tau_w e_m) \frac{\gamma}{P_s E_m}, \tag{20}$$

where the subscript w means a full width at half-maximum of the polarization current peak. If we could estimate the coefficient $(\tau_w e_m)$ in (20) on the basis of the present model, we may utilize it to evaluate the rotational viscosity as was recently proposed by Kimura *et al.*[5] The validity for it will be also discussed in the next section together with some examples of polarization current.

§3. NUMERICAL RESULTS AND DISCUSSIONS

In this section we shall show some numerical results for a step-like applied electric field together with a discussion of them. In the following computations, we used a conventional finite difference method to solve Equations (15), (17a), and (17b), and assumed $G^0 = G^d = G$ and put $\Phi_0 = \Phi_d$ to 1 deg in order to compare the present results with the previous work.[2,5] In addition, the inherent chirality Q, which is equivalent to a polarity of surface anchoring,[8] was put to 0. The initial value of $\Phi(\zeta,\tau)$, or $\Phi(\zeta,0)$, is set to a spatially homogeneous solution of Equations (15)–(17) with $e(t) = 0$. If we neglect the elastic restoring torque $\partial^2\Phi/\partial\zeta^2$ as well as the polarization electric field e_p, the present model is reduced to a spatially homogeneous model without a dielectric anisotropy.

First of all, we shall show several numerical results for the strong anchoring limit, or $G \to \infty$ and $\alpha > 0$. The results for $e_m = 20$ are shown in Figure 2(a)–(c) for various Λ. Therein $\Phi(1/2)$ represents the value of Φ at $\zeta = 1/2$. From these, an increase of Λ is found to result in a decrease of the polarization current peak value. In other words, the polarization electric field has a tendency to make an effective stiffness of SmC* liquid crystals increase as was noted in the previous section. In addition, it should be noted here that the peak position of I_p is shifted forwards as if the SmC* sample had a positive dielectric anisotropy.[5] Therefore, judging from this finding, it seems to be inappropriate to detect the dielectric anisotropy of SmC* only based on a profile of the switching current I_p.[5] This point

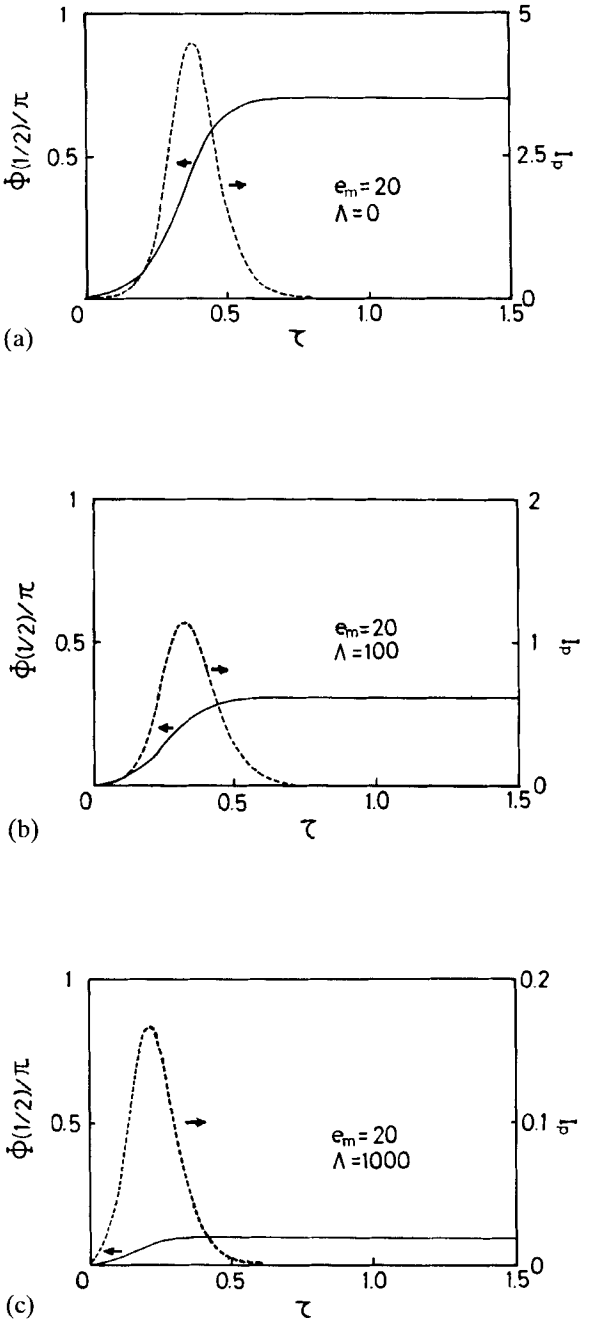

FIGURE 2 The time dependence of polarization switching currents and the rotation angles at the middle point $\zeta = 1/2$ on Λ. Here $e_m = 20$: a) $\Lambda = 0$; b) $\Lambda = 100$; c) $\Lambda = 1000$.

will be seen in Figure 3 for $e_m = 50$ in more detail. Therein an asymmetry coefficient r of I_p is specified by the following quantity

$$r = \frac{\tau_{p2} - \tau_{p1}}{\tau_{p2} + \tau_{p1}} = \frac{\tau_{p2} - \tau_{p1}}{\tau_w}, \tag{21}$$

where the definitions of τ_{p1} and τ_{p2} are presented by the inset in Figure 3; here $\tau_w = \tau_{p1} + \tau_{p2}$. From this result, one finds that the polarization electric field plays a role to shift the peak position of I_p forwards. Next a few examples of the e_m dependence of the dynamic behavior are presented in Figure 4(a) and (b) for $\Lambda = 100$ (see also Figure 2(b).). With increasing e_m, one finds that the response becomes more rapid, and that the peak position of I_p is shifted forwards as is to be usually expected. At the same time, τ_w is found to be decreased with increasing e_m. In Figures 5 and 6, let us summarize the dependences of τ_p (peak position) and τ_w on $1/e_m$ for $\Lambda = 0$ and 100. Here τ_p is defined as the time to attain a maximum after the field application. In addition, for comparison, we presented the result for $K = \Lambda = 0$, which corresponds to those derived by Xue Jiu-zhi *et al.*[2] and Kimura *et al.*[5] if we put the dielectric anisotropy to 0 in their model. From these results, one may find that both τ_p and τ_w are no longer linearly proportional to $1/e_m$ for $K \neq 0$. Only for a spatially homogeneous model with $K = \Lambda = 0$, we find the following linear relation from Figure 6.

$$\tau_w = 1.8/e_m. \tag{22}$$

This result just corresponds to $t_w = 1.76\gamma/P_sE_m$ numerically derived by Kimura *et al.*[6] who concluded that this relation may be applicable over a relatively wide range of the dielectric anisotropy. As can be seen from curves a and b in Figure 6, however, the above relation has to be somewhat modified when the elastic restoring

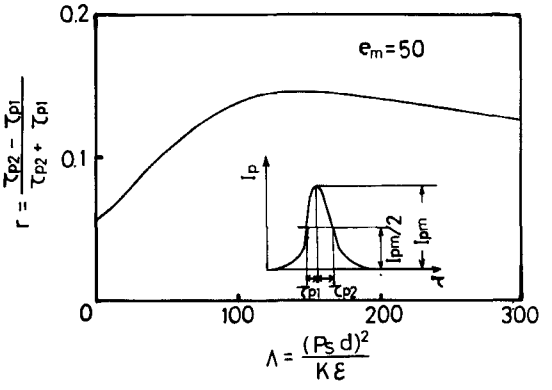

FIGURE 3 The dependence of asymmetry of polarization switching current on Λ.

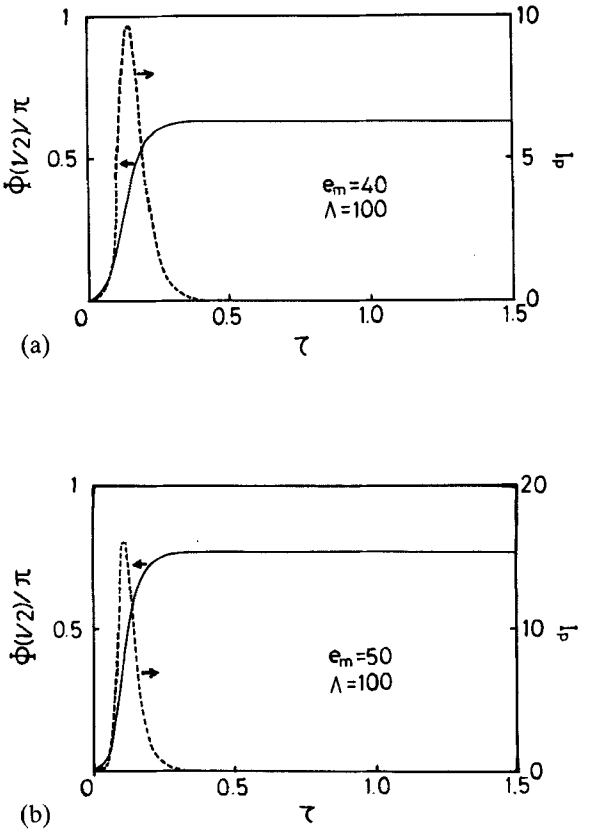

FIGURE 4 The time dependence of polarization switching currents and the rotation angles at the middle point $\zeta = 1/2$ on e_m. Here $\Lambda = 100$. See also Figure 2(b): a) $e_m = 40$; b) $e_m = 50$.

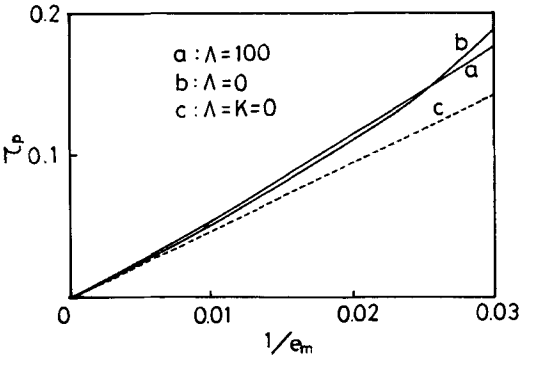

FIGURE 5 The $1/e_m$ dependence of the peak position of polarization switching current on Λ. Here the dashed curve c is for $\Lambda = K = 0$, i.e., for a spatially homogeneous model.

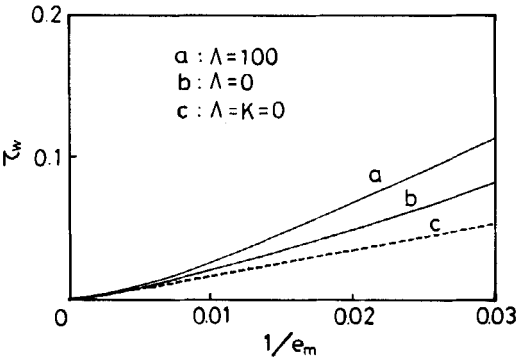

FIGURE 6 The $1/e_m$ dependence of the full width at the half-maximum of polarization switching current on Λ. Here the dashed curve c is for $\Lambda = K = 0$ as the same with Figure 5.

force and the polarization electric field cannot be neglected. In Figure 7, the dependence of $e_m\tau_w$ on Λ is presented for $e_m = 50$. From this result, one can easily see the significance of the polarization electric field as well as the elastic restoring force. Remarkably, even for $\Lambda = 0$, such a linear relationship as (22) does not hold because of the elastic restoring force. In fact, for $e_m = 50$, the elastic torque $\partial^2\Phi/\partial\zeta^2 \sim \pi^2\Phi$ may be estimated by about 5 times smaller than the electric torque $e_m\sin\Phi \sim e_m\Phi$. For this example, one may find an almost linear relationship as $\tau_w = 3.6/e_m$ between $100 < \Lambda < 300$, which means that the rotational viscosity may be overestimated by about twice if we use (22) under such conditions. Of course, since τ_w does not linearly depend on $1/e_m$ as shown in Figure 6, this relation should be somewhat modified for the other values of e_m.

Second we shall consider the dynamic behavior with weakly anchored boundaries which seem to be more fascinating for practical applications of SmC*. In the following computations we put $\alpha = 10$. The effect of the polarization field also may be reduced in comparison with the strongly anchored case studied above since

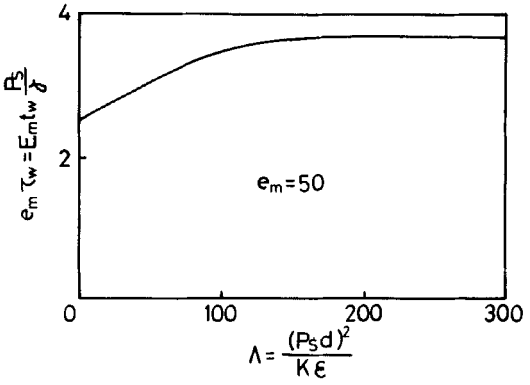

FIGURE 7 The dependence of $e_m\tau_w = E_m t_w P_s/\gamma$ on Λ for $e_m = 50$.

the spatial inhomogeneity of the c-director will be reduced by a possible rotation of the boundary molecules. In Figures 8(a) and (b), let us show the polarization switching current for various anchoring strengths G with $e_m = 50$ and $\Lambda = 0$ (a), $\Lambda = 100$ (b). Here we also presented the result for G = 0, i.e., a spatially homogeneous model. From these results, the anchoring strength is also found to critically affect the profiles of I_p. As a whole, the anchoring effect at the boundaries has a tendency to shift the peak of I_p backwards in contrast to the effect of the polarization field previously noted. Remarkably for relatively strong anchoring, secondary peaks of polarization currents are found for both $\Lambda = 0$ and 100. Such secondary peaks are explained as a result of an acceleration by the surface anchoring torque as will be explored in the next section. It should be noted here that the secondary peak for $\Lambda = 100$ appears much sooner than that for $\Lambda = 0$. That is, the molecules tend to rotate more cooperatively for $\Lambda = 100$ than for $\Lambda = 0$. In addition, for G $\geqq$ 300 in these results, the c-director of boundary molecules did not pass the potential barrier of $f_s^{0,d}$ at $\Phi = \pi/2$ and could not be finally inverted. This tendency suggests that there exists a certain threshold value of G necessary to realize bistable operation under a fixed applied electric field. Different from the strongly anchored case, r is found to take negative values in analogous to the

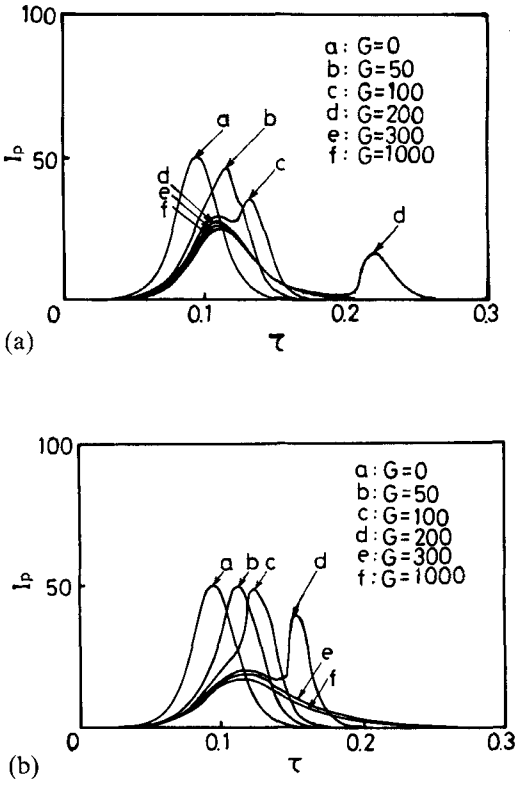

FIGURE 8 The time dependence of polarization switching current on the boundary anchoring strength G. Here $\alpha = 10$ and $e_m = 50$: a) $\Lambda = 0$; b) $\Lambda = 100$.

previous findings under a sinusoidal electric field.[8] Therefore, as was previously noted, it seems to be implausible to determine the sign of the dielectric anisotropy only from the profile of I_p contradicting the proposal by Kimura *et al.*[5]

§4. CONCLUDING REMARKS

We have presented a simple elastic model of SmC* liquid crystals to study their dynamic properties under an electric field and presented some numerical results to clarify the effects of polarization electric field on them in the surface-stabilized geometry. From the present results, as a whole, we found that the polarization electric field makes the full width at the half-maximum of the polarization current broaden, and that it considerably relaxes the dynamic response of SmC*. Therefore if we neglect this effect to estimate the rotational viscosity, its value may be over-estimated as can be seen from Figure 6. Moreover even if we assume $\Lambda = 0$ in Equation (16), we could not find a linear relationship between τ_w and $1/e_m$ for a strongly anchored case because of the elastic restoring force. Therefore as one may roughly estimate that the elastic contribution $\partial^2\Phi/\partial\zeta^2 \sim \pi^2\Phi$ and $e_m \sin\Phi \sim e_m\Phi$, it seems to be plausible to ignore the elastic restoring force in (15) only for $e_m >> \pi^2 \sim 10$.

To conclude this work, it may be worthwhile to present a few examples of the spatio-temporal behavior of the polarization electric field $e_p(\zeta,\tau)$ and the director orientation $\Phi(\zeta,\tau)$. In Figure 9(a) and (b), let us first depict time progress of the profiles of $e_p(\zeta,\tau)$ and $\Phi(\zeta,\tau)$, respectively for $e_m = 50$ and $\Lambda = 100$ with strongly anchored boundaries. In Figure 9(a), one can confirm that the magnitude of the induced polarization field e_p near the boundaries is almost comparable with the externally applied electric field $e = -e_m$ or larger. Near the boundaries, e and e_p have a same direction, whereas they have opposite directions in the middle region. Therefore while the SmC* molecules near the boundaries may experience a stronger field to rotate them towards $\Phi \sim \pi$ direction than the externally applied one, the inner molecules experience a much weaker field than the externally applied field. Remarkably, in this example, the externally applied field is almost canceled by the induced polarization field near the middle of the sample. Hence, an acceleration of the *c*-director will be considerably reduced as is presently found. Consequently the full width of the half-maximum of polarization current I_p will be broadened as the coupling parameter Λ becomes large. Alternatively this may result in a positive correlation between the apparent rotational viscosity and the spontaneous polarization. In fact, recently, certain positive correlation between them was experimentally confirmed by Dubal *et al.*[11] in an enantiomeric mixture. In addition, more recently, Chandani *et al.* found a large rotational viscosity for relatively high spontaneous polarization.[12] Therefore it seems to be significant to compare the present result with experimental data when determining the rotational viscosity. Next we shall consider a weakly anchored case. The numerical results $e_p(\zeta,\tau)$ and $\Phi(\zeta,\tau)$ of for $e_m = 50$, $\Lambda = 100$, $G = 200$, and $\alpha = 10$ are shown in Figure 10(a) and (b), respectively (see also Figure 8(b).). This behavior may be explained as follows.

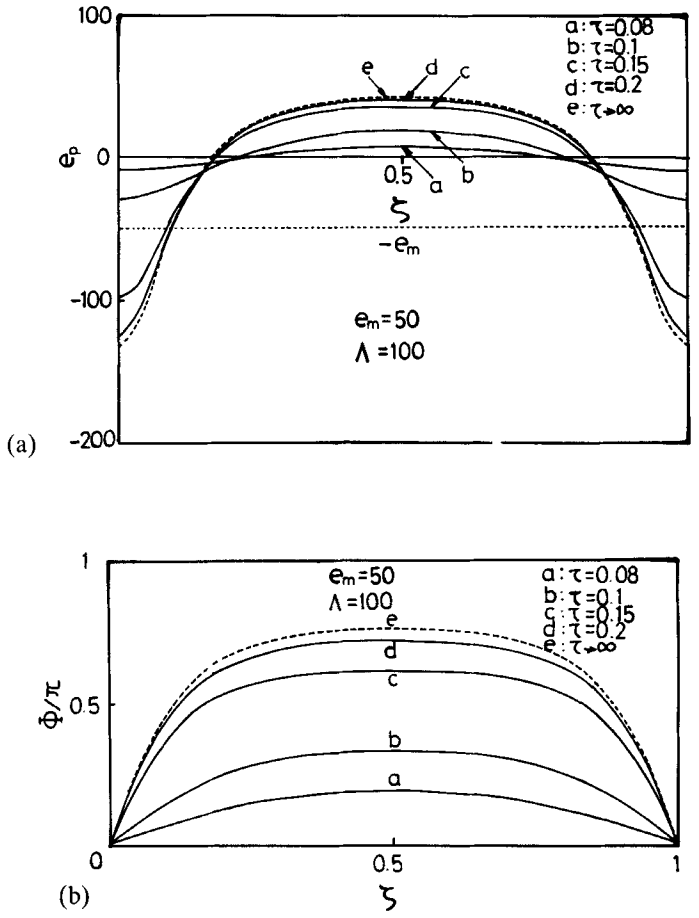

FIGURE 9 Spatio-temporal behavior for strongly anchored cases: a) $e_p(\zeta,\tau)$; b) $\Phi(\zeta,\tau)$.

First the molecules near the boundaries rotate later compared with the inner molecules because of the anchoring torque $-\partial f_s/\partial\Phi < 0$ which prevents rotation of the SmC* molecules. Therefore the rotation of the boundary molecules are mainly driven by that of the inner bulk molecules. This process corresponds to the first peak in I_p in Figure 8(b). However, as soon as the border molecules pass through the potential barrier at $\Phi = \pi/2$, they will be accelerated because of the anchoring torque $-\partial f_s/\partial\Phi > 0$ and then be rotated rather than the inner molecules. This acceleration results in the secondary peak in I_p. Thus the inversion will be accomplished after these two steps. In Fig. 8(a) and (b), the secondary I_p peak for $\Lambda = 100$ appears much sooner than that for $\Lambda = 0$. This trend is also considered as a result of an increase of the apparent elastic constant as may be seen from the above explanation. As can be seen from these behaviors, the effects of the polarization field and the surface anchoring are considered to crucially bear on the dynamic behavior of SSFLCs.

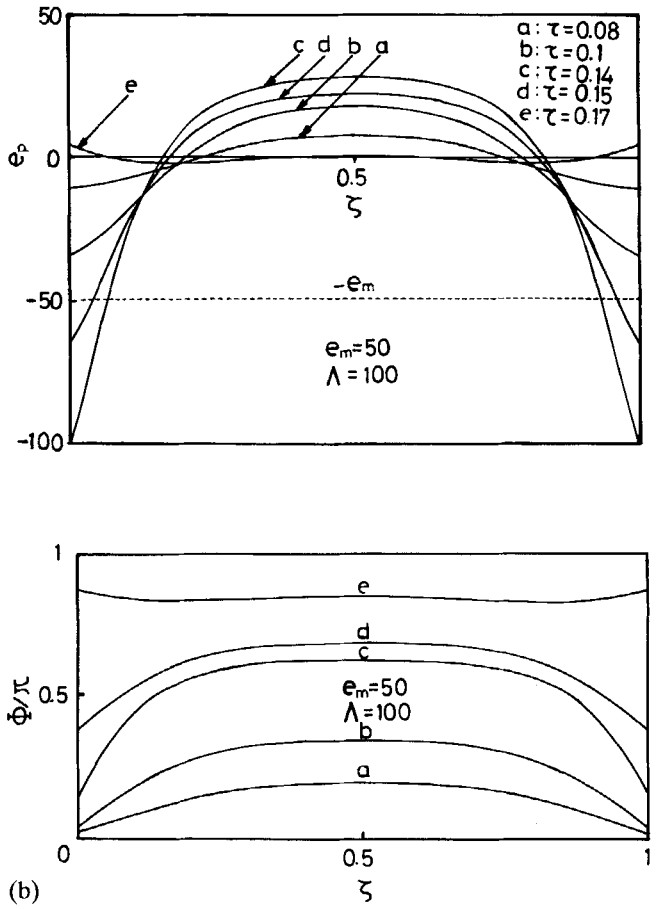

FIGURE 10 Spatio-temporal behavior for weakly anchored cases. Here $\alpha = 10$ and $G = 200$; a) $e_p(\zeta,\tau)$; b) $\Phi(\zeta,\tau)$.

Acknowledgement

The present author wishes to thank to Professor T. Akahane for the encouragement throughout the present study. He also greatly appreciates to Professor F. M. Leslie and his colleagues at the Strathclyde University for their discussions on continuum theory and kind hospitality during his stay in Glasgow.

This work is supported in part by the Visiting Researcher Scholarship from the Ministry of Education of Japan.

References

1. P. G. Amaya, M. A. Handschy, N. A. Clark, *Opt. Eng.*, **23,** 261 (1984).
2. Xue Jiu-zhi, M. A. Handschy and N. A. Clark, *Ferroelectrics*, **73,** 305 (1987).
3. I. Dahl, S. T. Lagerwall and K. Skarp, *Phys. Rev. A*, **36,** 4380 (1987).
4. S. Nonaka, K. Ito, M. Isogai and M. Odamura, *Jpn. J. Appl. Phys.*, **26,** 1609 (1987).
5. S. Kimura, S. Nishiyama, Y. Ouchi, H. Takezoe and A. Fukuda, *Jpn. J. Appl. Phys.*, **26,** L255 (1987).

6. M. Nakagawa and T. Akahane, *J. Phys. Soc. Jpn.*, **55,** 1516 (1986).
7. M. Nakagawa and T. Akahane, *J. Phys. Soc. Jpn.*, **55,** 4429 (1986).
8. M. Nakagawa and T. Akahane, *Jpn. J. Appl. Phys.*, **27,** 456 (1988).
9. K. Okano, *Jpn. J. Appl. Phys.*, **25,** L846 (1986).
10. Y. Ouchi, H. Takezoe and A. Fukuda, *Jpn. J. Appl. Phys.*, **26,** 1 (1987).
11. H. Dubal, C. Escher and D. Ohlendorf, 1st International Symposium on Ferroelectric Liquid Crystals, O-8, Bordeaux-Archon, 1987.
12. A. D. L. Chandani, Y. Ouchi, H. Takezoe and A. Fukuda, *Jpn. J. Appl. Phys.*, **27,** L276 (1988).